

Efficient photovoltage multiplication in carbon nanotubes

Leijing Yang^{1,2,3†}, Sheng Wang^{1,2†}, Qingsheng Zeng^{1,2}, Zhiyong Zhang^{1,2}, Tian Pei^{1,2}, Yan Li^{1,4} and Lian-Mao Peng^{1,2*}

Carbon nanotubes are direct-bandgap materials that are not only useful for nanoelectronic applications^{1,2}, but also have the potential to make a significant impact on the next generation of photovoltaic technology^{3–5}. A semiconducting single-walled carbon nanotube (SWCNT) has an unusual band structure, as a result of which high-efficiency carrier multiplication effects have been predicted and observed^{6,7} and films of SWCNTs with absorption close to 100% have been reported⁸. Other features that are also important for photovoltaic applications include high mobility^{9,10} and the availability of ohmic contacts for both electrons^{11,12} and holes¹³. However, the photovoltage generated from a typical semiconducting SWCNT is less than 0.2 V, which is too small for most practical photovoltaic applications. Here, we show that this value may be readily multiplied by using virtual contacts at the carbon nanotube. In one example, more than 1.0 V is generated from a 10- μm -long carbon nanotube with a single-cell photovoltage of ~ 0.2 V.

In a typical photovoltaic device, a built-in field is essential for the efficient separation of photon-excited electron-hole pairs and for the observation of photovoltaic effects¹⁴. In carbon nanotube (CNT) diodes, such a built-in field is usually provided by forming a p-n junction through chemical¹⁵ or electrostatic doping and making use of split gates^{7,16,17}. A Schottky barrier formed between a metal electrode (for example, titanium) and a semiconducting single-walled CNT (SWCNT) can also provide the required field for separating electrons and holes. However, the creation of the Schottky barrier reduces the maximum achievable photovoltage¹⁸. Here, we consider a recently developed CNT diode device: a barrier-free bipolar diode¹⁹. This CNT diode consists of an intrinsic semiconducting SWCNT that is asymmetrically contacted with palladium and scandium or yttrium (Fig. 1a). It has been shown that carriers can be injected (without barrier) into the CNT valence band from the palladium electrode¹³ and into the conduction band from the scandium and yttrium electrodes^{11,12}. In principle, because there is neither a Schottky barrier nor a sharp p-n junction in such a diode, the maximum photovoltage achievable is ultimately determined by the bandgap of the CNT, allowing the creation of a highly efficient CNT light-emitting diode²⁰.

Diode devices were fabricated with scandium and palladium electrodes asymmetrically contacted to the CNT (Fig. 1a). This asymmetrically contacted semiconducting SWCNT had typical diode rectifying I - V characteristic (Fig. 1b) in the dark. However, when illuminated, electron-hole pairs were created in the CNT, which were then separated by the built-in electric field in the diode, yielding a photocurrent, I_{sc} . Photocurrent spectroscopy experiments were carried out that demonstrated a clear maximum corresponding to the interband absorption of the CNT (Supplementary Fig. S2).

Under low illumination conditions, the total current in the channel was determined by the balance between the dark current and the light-generated current, and total current $I(V)$ could be approximated as an illumination-dependent downshift of the dark current (Fig. 1b, red curve). The key performance metric for a solar cell is the power conversion efficiency, which is defined as $\eta = (I_M \times V_M)/P_{in} = (FF \times I_{sc} \times V_{oc})/P_{in}$, where I_M and V_M describe the bias point at which the power generation reaches a maximum, I_{sc} and V_{oc} are the short-circuit current and open-circuit voltage, respectively, P_{in} is the incident power density and FF is the fill factor. For the device shown in Fig. 1d, η is estimated to be $\sim 0.11\%$. Although both the FF and η values look very low when compared with those for a silicon-based solar cell¹⁴, they are of the same order of magnitude as that obtained from an almost perfect CNT diode²¹ fabricated using electrostatic doping on a suspended CNT. The low value of η achieved here is largely due to the fact that the diameter of the CNT and thus the absorption cross-section is extremely small for a single-CNT-based diode. The actual quantum efficiency of the CNT diode is also estimated after taken into account the CNT absorption cross-sections, suggesting a much higher efficiency (details are given in the Supplementary Information).

For most practical applications, the photovoltage generated from a single CNT diode is too small. In principle, the photovoltage of a solar module may be made much larger than that of a single cell by connecting several cells in series. In silicon-based solar cells, the typical size of a cell is 10 cm \times 10 cm, with $V_{oc} = 0.5$ – 0.6 V, and about 30 cells are connected externally to produce an output voltage of ~ 12 V (ref. 22). Alternatively, a cascade or tandem cell structure, which is simply a stack of solar cells, may be used. These tandem cells are, however, expensive to make and are mainly being developed for use in space where efficiency is paramount¹⁴. Here, we show that a homojunction tandem cell may be fabricated, based on CNTs, by using a simple doping-free approach (Fig. 2a). The key to this approach is the introduction of a local virtual contact to the CNT. This contact is virtual in the sense that it is not intended to be connected to the external circuit. Instead, this virtual contact provides an internal parallel path for electronic transport, and acts as a smart gate that modulates the potential distribution in the CNT channel, forming a p-n junction beneath the virtual contact (Fig. 2b).

A typical virtual contact is composed of overlapping scandium (or yttrium) and palladium pads (Fig. 2a). Because the Fermi levels of scandium and palladium pads are aligned to the CNT conduction and valence bands, respectively^{11–13}, the virtual contact serves to provide an alternative local route for the carriers (in parallel with the CNT channel) to move from the conduction band of the

¹Key Laboratory for the Physics and Chemistry of Nanodevices, Peking University, Beijing 100871, China, ²Department of Electronics, Peking University, Beijing 100871, China, ³Academy for Advanced Interdisciplinary Studies, Peking University, Beijing 100871, China, ⁴College of Chemistry and Molecular Engineering, Peking University, Beijing 100871, China; [†]These authors contributed equally to this work. *e-mail: lmpeng@pku.edu.cn

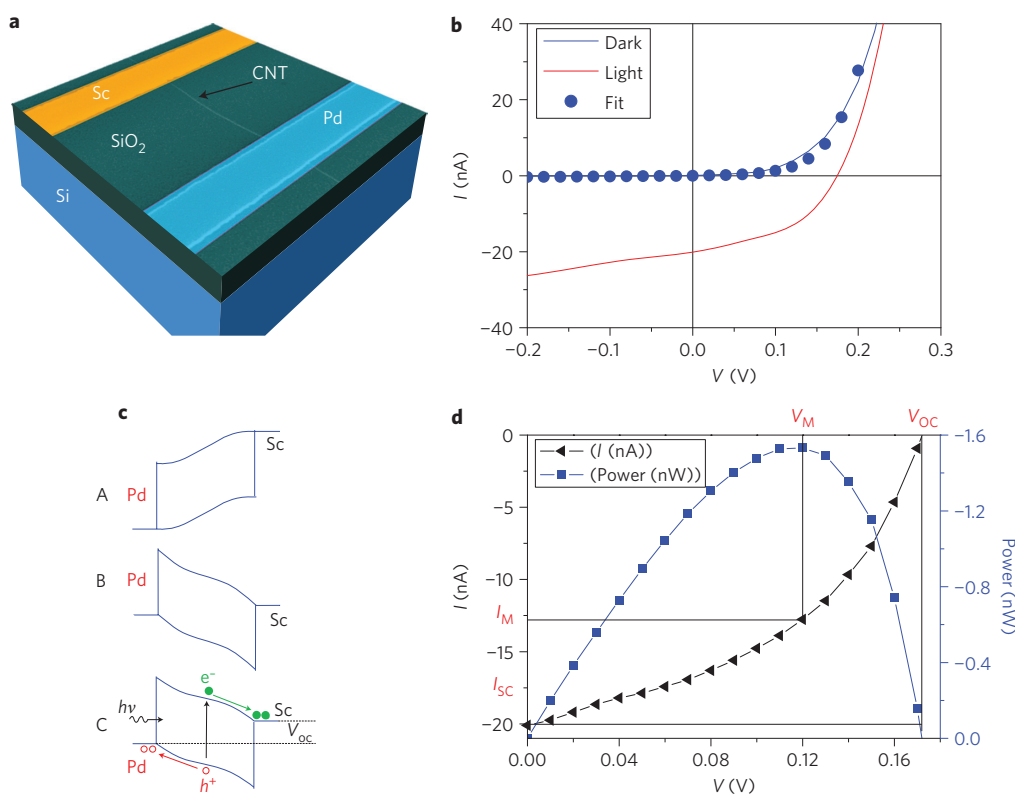


Figure 1 | Structure and performance of a CNT-based photovoltaic device. **a**, Superimposed scanning electron microscopy image and device structure schematic showing a SWCNT-based photovoltaic device. Diameter of SWCNT, 1.7 nm; thickness of scandium and palladium electrodes, 60 nm. **b**, Experimental and fitted I - V characteristic in the dark (blue) and under illumination (red) measured for a device with a channel length of 1.0 μm and light intensity of 90 kW cm^{-2} . **c**, Energy band diagrams of the CNT photovoltaic device, with large forward bias (A), zero or small bias (B) and under illumination (C). **d**, I - V (black) and output power (blue) characteristics for the same device as in **b**, illustrating the key parameters related to the performance of the device: $I_M = 12.8$ nA, $V_M = 0.12$ V, $V_{OC} = 0.17$ V, $I_{SC} = 19.8$ nA and $FF = 0.42$.

CNT to the valence band (Fig. 2b). Although a typical single CNT cell may generate a photovoltage of ~ 0.12 – 0.14 V, the introduction of a virtual contact (Fig. 2a) roughly doubles the photovoltage (Fig. 2c). A simple comparison with conventional solar cells might suggest that the operation principle of the virtual scandium/palladium contact is the same as for conventional solar cells connected in series, but a careful consideration reveals that the fundamental physics is very different. In conventional solar cells, the series connection is made between two physically separated regions with different chemical potentials, for example, between a heavily p-doped region and a heavily n-doped region. In the present device, the CNT is intrinsic and the connection made by the virtual contact is between two different parts of the same CNT with a single chemical potential. The key idea behind the working principle of the virtual contact is that the connection is made to different energy levels rather than locations. The scandium is connected to the conduction band, and the palladium is connected to the valence band, and photovoltage multiplication results mainly from this energy-selective connection.

When forming the virtual scandium/palladium contact, the scandium and palladium pads are brought together, creating an electron-rich region near the scandium pad and hole-rich region near the palladium pad, along the CNT channel. The effect of the virtual contact on the CNT is to introduce a potential valley in the conduction band near the scandium pad and a hill in the valence band near the palladium pad. The potential valley and hill are formed automatically, because in the virtual scandium/palladium, contact surface charges must be redistributed such that the potential of the entire metallic scandium/palladium contact

remains constant. These non-uniformly distributed charges near the CNT then align the local conduction band of the CNT towards the Fermi level of the scandium pad, and the valence band towards the Fermi level of the palladium pad (Fig. 2b). The virtual contact therefore creates physically separated electron and hole regions. These separated electrons and holes in the CNT can either tunnel through the bandgap or enter into the virtual scandium/palladium contact to maintain the current at a small and reverse bias. At open circuit, the voltage of the scandium electrode (to the right of Fig. 2b) will be raised by V_{OC} with respect to that of the virtual scandium/palladium electrode, whereas the palladium electrode (to the left of Fig. 2b) will be lowered by V_{OC} . The total open-circuit voltage is thus doubled (Fig. 2c). To investigate the effect of the virtual scandium/palladium contact pads on transport in the CNT tandem cell, a new device was fabricated in which the two virtual scandium and palladium pads were initially separated, and no photovoltage multiplication was observed (Supplementary Fig. S3a). When the two scandium and palladium pads were externally connected, photovoltage multiplication was then observed, without (Supplementary Fig. S3e) and with (Supplementary Fig. S3c) the CNT channel between the scandium and palladium pads. This experiment clearly demonstrates that the virtual scandium/palladium contact alone can result in photovoltage doubling, but with an additional CNT channel the efficiency is higher, leading to a much larger photocurrent.

Because the current passing through several CNT cells in series must be the same, the total module current is limited by the constituent cell with the smallest current. The short-circuit current of the module is therefore lower than that of any constituent cells

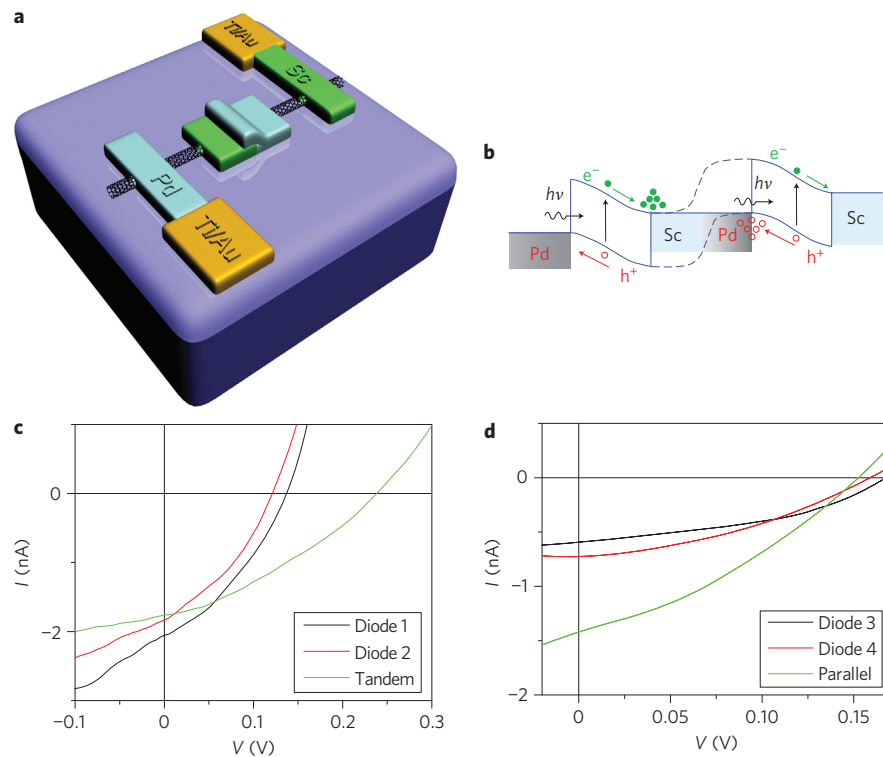


Figure 2 | Structure and performance of CNT-based double-cell photovoltaic modules. **a**, Schematic illustrating a CNT photovoltaic module with two cells connected in series. **b**, Energy band diagram illustrating the excitation and accumulation of electrons and holes under illumination. **c**, I - V characteristics measured for two individual photovoltaic cells fabricated on a SWCNT with a diameter of 2.1 nm and for a photovoltaic module consisting of the two cells connected in series. Although the short-circuit current of the module is slightly smaller than that from individual cells, the open-circuit voltage is almost doubled. **d**, I - V characteristics measured for two individual photovoltaic cells fabricated on a SWCNT with a diameter of 1.6 nm and for the photovoltaic module consisting of the two cells connected in parallel. The open-circuit voltage of the module is slightly smaller than that for individual cells, but the short-circuit current is almost doubled.

(Fig. 2c). However, the CNT module current may be readily increased by connecting several CNTs in parallel. Although the open-circuit voltages for the multiple CNT module and its constituent parallel cells are about the same, with the module photovoltage being limited mainly by the cell with the lowest photovoltage, the total module current is indeed roughly doubled for a double CNT module consisting of two cells connected in parallel (Fig. 2d).

The working principle for doubling the cell photovoltage in CNTs may readily be generalized to CNT photovoltaic modules with more cells to generate higher photovoltage. Figure 3a presents a general CNT photovoltaic module structure composed of m sub-modules connected in parallel, each consisting of n cells connected in series. For a perfect module, the total open-circuit voltage is nV_{oc} and the short-circuit current is mI_{sc} , where V_{oc} and I_{sc} are the open-circuit voltage and short-circuit current, respectively, of a single cell. An optical image showing a real device consisting of four cells connected in series is given in Fig. 3b, and the corresponding I - V curves are given in Fig. 3c. Although a single cell produces a photovoltage of ~ 0.23 V, the double-cell module produces 0.41 V, the triple cell module 0.59 V, and quadruple cell module 0.84 V. In total, 30 independent modules were fabricated on the same CNT, and the average results for these are given in Fig. 3d (see Supplementary Fig. S4 for a complete photovoltage data set for these devices). This figure shows clearly that a linear relation exists between the open-circuit voltage of the module and the number of cells connected in series within the module, suggesting that extremely low losses arise from introducing the virtual contacts to the cascaded constituent CNT cells. The open-circuit voltage follows a linear relationship very closely, but the short-circuit current is not a constant as expected and indeed differs substantially from module to module depending on the

illumination conditions. Figure 3c shows, for the single-, double- and triple-cell modules, that the short-circuit current remains essentially at the same level, decreasing slightly as more cells are introduced into the module. However, the short-circuit current of the module drops significantly when the fourth cell is included in the module. Careful examination of the experimental conditions reveals that this sudden drop in the short-circuit current is not due to the device itself. Instead, this is largely due to the fact that the intensity of the illumination spot is not uniform, showing a very strong drop in intensity at the edge of the spot.

Only the homojunction tandem cell is demonstrated here on a CNT, but a general tandem cell may in principle be fabricated in the same way on a semiconducting CNT with varying diameter or energy bandgap, starting with smaller diameters and moving towards larger cells²³. It should be noted that in the conventional tandem cell the connection between adjacent cells is usually realized via tunnelling layers composed of heavily n- and p-doping layers, which increase scattering, reducing the current and degrading or damaging the cell at high temperature when dopants start to diffuse. As the CNT tandem cell structure discussed here is fabricated using a doping-free approach, the function of the cell is not dependent on dopants. The device may thus be used at high temperature without suffering dopant-diffusion-induced failure. The device can also work at extremely low temperatures, because there is no issue with frozen dopant. In other words, our device may, in principle, work in extreme environments—in space, extremely hot desert conditions, or in an extremely cold polar area²⁴.

As-grown CNTs usually contain both semiconducting and metallic CNTs, and are not suitable for photovoltaic applications. However, rapid progress has been made in recent years in nanotube

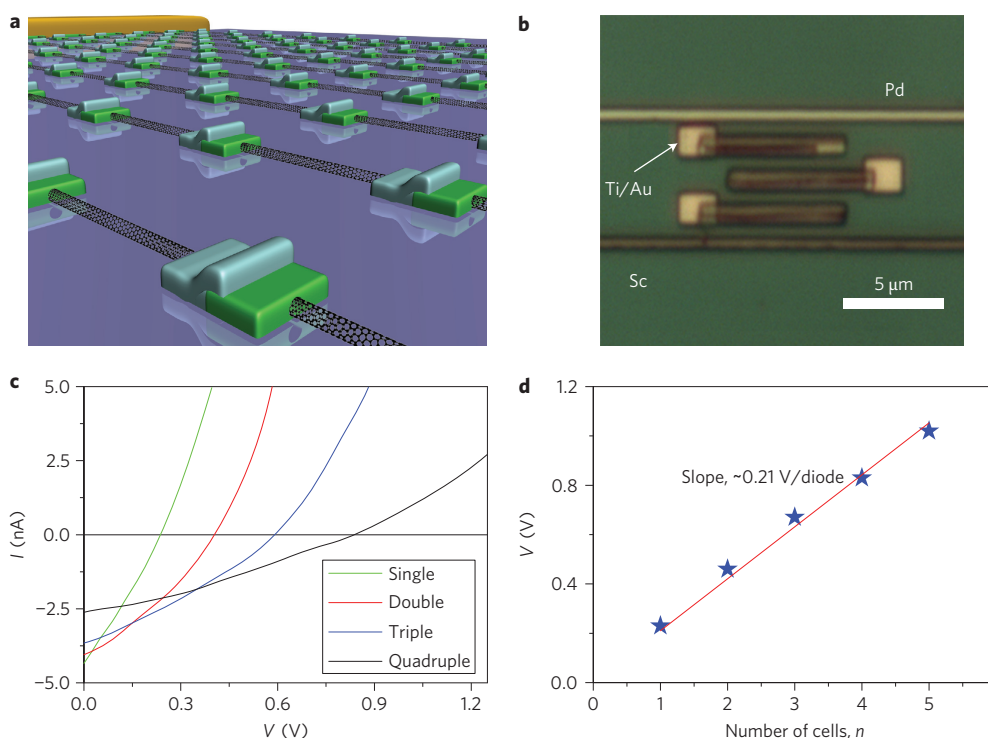


Figure 3 | Structure and characteristics of cascaded CNT photovoltaic modules. **a**, Schematic of a general CNT photovoltaic module consisting of m SWCNT-based tandem cells, each with n cells connected in series. The total open-circuit voltage is expected to be n times that of a single photovoltaic cell, and the short-circuit current m times that of a single cell. **b**, Optical microscope image showing a real test tandem photovoltaic device with $m = 1$ and $n = 4$. **c**, Corresponding I - V characteristics for the tandem cells with one (green), two (red), three (blue) and four (black) individual cells connected in series during the measurements. **d**, Statistic results measured from a total of 30 photovoltaic modules with $m = 1$ and $n = 1$ (single), 2 (double), 3 (triple), 4 (quadruple) and 5 (quintuple). All devices are fabricated on a SWCNT (diameter, ~ 1.5 nm), and measurements were carried out under an incident power P_{in} of 9.7 kW cm^{-2} . The open-circuit voltage follows a perfect linear relationship with n , yielding 0.21 V/diode .

separation. High-purity (99%) semiconducting CNTs have now been obtained^{25–27}, providing a good opportunity for the application of the photovoltage multiplication technique developed here in real devices.

Methods

The ultralong SWCNTs used in this work were grown by chemical vapour deposition (CVD) on silicon wafers, which were covered with 500-nm-thick SiO_2 (ref. 28). The electronic measurement pads used in this work were composed of titanium/gold layers (with 5 nm/45 nm), which were patterned and formed by means of electron-beam lithography and evaporation. The CNT diode was fabricated with 60 nm scandium and palladium electrodes patterned on its two ends using the same process as used for the titanium/gold electrodes. The device channel was fully covered with 180 nm polymethyl methacrylate (PMMA). Semiconducting SWCNTs were identified via electric field-effect measurements.

The diameters of the CNTs were measured using atomic force microscopy (Veeco Company, DI 3100) and characterized by Raman experiments (Jobin Yvon/Horiba company; Supplementary Fig. S1). Raman spectroscopy measurements were carried out using lasers with wavelengths of $\lambda = 633 \text{ nm}$ and 785 nm , and all spectra were collected using a microscope objective ($\times 100$) lens. A typical integration time of 30 s was used for collecting a spectrum.

Optoelectric measurements of CNT devices were performed on a probe station attached to the Raman system. The power of the focused laser beam (785 nm) on the device could be varied from 0 to 30.5 mW. All electronic transport measurements were carried out using a Keithley 4200 semiconductor analyser at room temperature.

Received 9 June 2011; accepted 25 August 2011;
published online 9 October 2011

References

- Charlier, J. C., Blase, X. & Roche, S. Electronic and transport properties of nanotube. *Rev. Mod. Phys.* **79**, 677–732 (2007).
- Javey, A. & Kong, J. (eds) *Carbon Nanotube Electronics* (Springer, 2009).
- Avouris, Ph., Freitag, M. & Perebeinos, V. Carbon-nanotube photonics and optoelectronics. *Nature Photon.* **2**, 341–350 (2008).
- Zhu, H. W., Wei, J. Q., Wang, K. L. & Wu, D. H. Applications of carbon materials in photovoltaic solar cells. *Solar Energy Mater. Solar Cells* **93**, 1461–1470 (2009).
- Chen, C., Lu, Y., Kong, E. S., Zhang, Y. F. & Lee, S. T. Nanowelded carbon-nanotube based solar microcells. *Small* **4**, 1313–1318 (2008).
- Nozik, A. J. Nanoscience and nanostructures for photovoltaics and solar fuels. *Nano Lett.* **10**, 2735–2741 (2010).
- Gabor, N. M., Zhong, Z. H., Bosnick, K., Park, J. & McEuen, P. L. Extremely efficient multiple electron-hole pair generation in carbon nanotube photodiodes. *Science* **325**, 1367–1371 (2010).
- Yang, Z. P., Ci, L. J., Bur, J. A., Lin, S. Y. & Ajayan, P. M. Experimental observation of an extremely dark material made by a low-density nanotube array. *Nano Lett.* **8**, 446–451 (2008).
- Durkop, T., Getty, S. A., Cobas, E. & Fuhrer, M. S. Extraordinary mobility in semiconducting carbon nanotube. *Nano Lett.* **4**, 35–39 (2004).
- Saito, R., Dresselhaus, G. & Dresselhaus, M. S. *Physical Properties of Carbon Nanotubes* (Imperial College Press, 1998).
- Zhang, Z. Y. *et al.* Self-aligned ballistic n-type single-walled carbon nanotube field-effect transistors with adjustable threshold voltage. *Nano Lett.* **8**, 3696–3701 (2008).
- Ding, L. *et al.* Y-contacted high-performance n-type single-walled carbon nanotube field-effect transistors: scaling and comparison with Sc-contacted devices. *Nano Lett.* **9**, 4209–4214 (2009).
- Javey, A., Guo, J., Wang, Q., Lundstrom, N. & Dai, H. J. Ballistic carbon nanotube field-effect transistors. *Nature Nanotech.* **5**, 27–31 (2010).
- Nelson, J. *The Physics of Solar Cells* (Imperial College Press, 2003).
- Zhou, C. W., Kong, J., Yenilmez, E. & Dai, H. J. Modulated chemical doping of individual carbon nanotube. *Science* **290**, 1552–1555 (2000).
- Lee, J. U., Gipp, P. P. & Heller, C. M. Carbon nanotube p-n junction diodes. *Appl. Phys. Lett.* **85**, 145–147 (2004).
- Mueller, T. *et al.* Efficient narrow-band light emission from a single carbon nanotube p-n diode. *Nature Nanotech.* **5**, 27–31 (2010).
- Avouris, Ph. *et al.* Carbon nanotube electronics and optoelectronics. *IEDM Tech. Digest* **04**, 525–529 (2004).
- Wang, S. *et al.* A doping-free carbon nanotube CMOS inverter-based bipolar diode and ambipolar transistor. *Adv. Mater.* **20**, 3258–3262 (2008).

20. Wang, S. *et al.* High-performance carbon nanotube light-emitting diodes with asymmetric contacts. *Nano Lett.* **11**, 23–29 (2011).
21. Lee, J. U. Photovoltaic effect in ideal carbon nanotube diodes. *Appl. Phys. Lett.* **87**, 073101 (2005).
22. Komp, R. J. *Practical Photovoltaics Electricity from Solar Cells* (AATEC Publications, 2001).
23. Yao, Y. *et al.* Temperature mediated growth of single-walled carbon nanotube intramolecular junctions. *Nature Mater.* **6**, 283–286 (2007).
24. Pei, T. *et al.* Temperature performance of doping-free top-gate CNT field-effect transistors: potential for low- and high-temperature electronics. *Adv. Funct. Mater.* **21**, 1843–1849 (2011).
25. Ghosh, S., Bachilo, S. M. & Weisman, R. B. Advanced sorting of single-walled carbon nanotubes by nonlinear density-gradient ultracentrifugation. *Nature Nanotech.* **5**, 443–450 (2010).
26. Liu, H., Nishide, D., Tanaka, T. & Kataura, H. Large-scale single-chirality separation of single-wall carbon nanotubes by simple gel chromatograph. *Nat. Commun.* **2**, 309-1-8 (2011).
27. Engel, M. *et al.* Thin film nanotube transistors based on self-assembled, aligned, semiconducting carbon nanotube arrays. *ACS Nano* **2**, 2445–2452 (2008).
28. Zhou, W. W. *et al.* Copper catalyzing growth of single-walled carbon nanotubes on substrates. *Nano Lett.* **6**, 2987–2990 (2006).

Acknowledgements

This work was supported by the Ministry of Science and Technology (grant nos 2011CB933002 and 2011CB933001), the Fundamental Research Funds for the Central Universities, and National Science Foundation of China (grant nos 61071013, 61001016, 51072006 and 60971003).

Author contributions

L.J.Y. and S.W. were responsible for the experimental work. Y.L. was responsible for the growth of the SWCNTs. L.M.P. conceived the project and supervised the research work. All authors discussed the results and contributed to the preparation of the manuscript.

Additional information

The authors declare no competing financial interests. Supplementary information accompanies this paper at www.nature.com/naturephotonics. Reprints and permission information is available online at <http://www.nature.com/reprints>. Correspondence and requests for materials should be addressed to L.M.P.